A Letters Journal Exploring the Frontiers of Physics

March 2016

EPL, **113** (2016) 60008
doi: 10.1209/0295-5075/113/60008

www.epljournal.org

Out-of-equilibrium fluctuations in stochastic long-range interacting systems

Shamik Gupta[1], Thierry Dauxois[2] and Stefano Ruffo[3]

[1] *Max-Planck Institute for the Physics of Complex Systems - Nöthnitzer Straße 38, D-01187 Dresden, Germany*
[2] *Univ. Lyon, ENS de Lyon, Univ. Claude Bernard, CNRS, Laboratoire de Physique - F-69342 Lyon, France*
[3] *SISSA, INFN and ISC-CNR - Via Bonomea 265, I-34136 Trieste, Italy*

received 26 December 2015; accepted in final form 5 April 2016
published online 13 April 2016

PACS 05.70.Ln – Nonequilibrium and irreversible thermodynamics
PACS 05.40.Ca – Noise

Abstract – For a many-particle system with long-range interactions and evolving under stochastic dynamics, we study for the first time the out-of-equilibrium fluctuations of the work done on the system by a time-dependent external force. For equilibrium initial conditions, the work distributions for a given protocol of variation of the force in time and the corresponding time-reversed protocol exhibit a remarkable scaling and a symmetry when expressed in terms of the average and the standard deviation of the work. The distributions of the work per particle predict, by virtue of the Crooks fluctuation theorem, the equilibrium free-energy density of the system. For a large number N of particles, the latter is in excellent agreement with the value computed by considering the Langevin dynamics of a single particle in a self-consistent mean field generated by its interaction with other particles. The agreement highlights the effective mean-field nature of the original many-particle dynamics for large N. For initial conditions in non-equilibrium stationary states (NESSs), we study the distribution of a quantity similar to dissipated work that satisfies the non-equilibrium generalization of the Clausius inequality, namely, the Hatano-Sasa equality, for transitions between NESSs. Besides illustrating the validity of the equality, we show that the distribution has exponential tails that decay differently on the left and on the right.

Copyright © EPLA, 2016

Introduction. – Fluctuations are ubiquitous in any physical system, and characterizing their behavior is one of the primary objectives of statistical physics. Fluctuations may originate spontaneously or may be triggered by an external force. When in thermal equilibrium, the system is unable to distinguish between the two sources of fluctuations, provided the fluctuations are small. As a result, the response of the system in thermal equilibrium to a small external force is related to the spontaneous fluctuations in equilibrium. The latter fact is encoded in the fluctuation-dissipation theorem (FDT), a cornerstone of statistical physics [1]. Intensive research on generalizing the FDT to situations arbitrarily far from equilibrium led to the formulation of a set of exact relations, clubbed together as the fluctuation relations (FRs). Besides quantifying the fluctuations, these relations constrain the entropy production and work done on the system [2]. Notable of the FRs are the Jarzynski equality [3] and the Crooks theorem [4] in which the system is driven far from an initial canonical equilibrium, and the Hatano-Sasa equality [5] that applies when the system is initially in a non-equilibrium stationary state (NESS).

Despite such a remarkable success on the theoretical front, observing in experiments the full range of fluctuations captured by the FRs has been limited almost exclusively to small systems. In a macroscopic open system comprising a large number (of the order of Avogadro number) of constituents, the dynamics is governed by the interaction of the environment with these many constituents, so that any macroscopic observable such as the energy shows an average behavior in time, and statistical excursions are but rare. A small system, on the contrary, is one in which the energy exchange during its interaction with the environment in a finite time is small enough so that large deviations from the average behavior are much more amenable to observation [6]. Molecular motors constitute a notable example of small systems involved in efficiently converting chemical energy into useful mechanical work inside living cells. Recent advances in experimental manipulation at the microscopic level led to experimentally

testing the FRs, *e.g.*, in an RNA hairpin [7], and in a system of microspheres optically driven through water [8].

In this work, we consider a macroscopic system with long-range interactions that is evolving under stochastic dynamics in the presence of a time-dependent external force. The stochasticity in the dynamics is due to the interaction of the system with the environment. Long-range interacting (LRI) systems are those in which the inter-particle potential decays slowly with the separation r as $r^{-\alpha}$ for large r, with $0 \leq \alpha < d$ in d dimensions [9].

Here, we study the out-of-equilibrium fluctuations of the work done on the system by the external force. We show that although constituted of a large number N of interacting particles, an effective single-particle nature of the dynamics, which becomes more prominent the larger the value of N is, leads to significant statistical excursions away from the average behavior of the work. The single-particle dynamics is represented in terms of a Langevin dynamics of a particle evolving in a self-consistent mean field generated by its interaction with other particles, and is thus evidently an effect stemming from the long-range nature of the interaction between the particles. For equilibrium initial conditions, we show that the work distributions for a given protocol of variation of the force in time and the corresponding time-reversed protocol exhibit a remarkable scaling and a symmetry when expressed in terms of the average and the standard deviation of the work. The distributions of the work per particle predict by virtue of the Crooks theorem the equilibrium free energy per particle. For large N, the latter value is in excellent agreement with the analytical value obtained within the single-particle dynamics, thereby confirming its validity. For initial conditions in NESSs, we study the distribution of the quantity Y appearing in the Hatano-Sasa equality (2). We show that the distribution decays exponentially with different rates on the left and on the right.

A recap of the fluctuation relations. – Consider a system evolving under stochastic dynamics, and which is characterized by a dynamical parameter λ that can be externally controlled. Let us envisage an experiment in which the system is subject to the following thermodynamic transformation: starting from the stationary state corresponding to a given value $\lambda = \lambda_1$, the system undergoes dynamical evolution under a time-dependent λ that changes according to a given protocol, $\{\lambda(t)\}_{0\leq t\leq\tau}; \lambda(0) \equiv \lambda_1, \lambda(\tau) \equiv \lambda_2$, over time τ. Only when λ changes slowly enough over a timescale larger than the typical relaxation timescale of the dynamics does the system pass through a succession of stationary states. On the other hand, for an arbitrarily fast variation, the system at all times lags behind the instantaneous stationary state. Dynamics at times $t > \tau$, when λ does not change anymore with time, leads the system to eventually relax to the stationary state corresponding to λ_2. In case of transitions between equilibrium stationary states, the Clausius inequality provides a quantitative measure of the lag at every instant of the thermodynamic transformation between the stationary state and the actual state of the system [10]. For transitions between NESSs, Hatano and Sasa showed that a quantity Y similar to dissipated work measures this lag [5], where Y is defined as

$$Y \equiv \int_0^\tau \mathrm{d}t\, \frac{\mathrm{d}\lambda(t)}{\mathrm{d}t} \frac{\partial \Phi}{\partial \lambda}(\mathcal{C}(t), \lambda(t)). \tag{1}$$

Here, $\Phi(\mathcal{C}, \lambda) \equiv -\ln \rho_{\rm ss}(\mathcal{C}; \lambda)$, and $\rho_{\rm ss}(\mathcal{C}; \lambda)$ is the stationary state measure of the microscopic configuration $\mathcal{C}$ of the system at a fixed λ. Owing to the preparation of the initial state and the stochastic nature of the dynamics, each realization of the experiment yields a different value of Y. An average over many realizations corresponding to the same protocol $\{\lambda(t)\}$ leads to the following exact result due to Hatano and Sasa [5]:

$$\langle e^{-Y} \rangle = 1. \tag{2}$$

In the particular case in which the stationary state at a fixed λ is given by the Boltzmann-Gibbs canonical equilibrium state, let us denote by $\Delta F \equiv F_2 - F_1$ the difference between the initial value F_1 and the final value F_2 of the Helmholtz free energy that correspond, respectively, to canonical equilibrium at λ_1 and λ_2. Then, if W is the work performed on the system during the thermodynamic transformation, the Jarzynski equality states [3] that

$$\langle e^{-\beta W} \rangle = e^{-\beta \Delta F}, \tag{3}$$

where β is the inverse temperature of the initial canonical distribution. Subsequent to the work of Jarzynski, a remarkable theorem due to Crooks related i) the distribution $P_{\rm F}(W_{\rm F})$ of the work done $W_{\rm F}$ during the forward process F, when the system is initially equilibrated at λ_1 and inverse temperature β, and then the parameter λ is changed according to the given protocol $\{\lambda(t)\}$, to ii) the distribution $P_{\rm R}(W_{\rm R})$ of the work done $W_{\rm R} = -W_{\rm F}$ during the reverse process R when the system is initially equilibrated at λ_2 and β, and then the parameter λ is changed according to the reverse protocol $\{\widetilde{\lambda}(t) \equiv \lambda(\tau - t)\}$. The theorem [4] states that

$$\frac{P_{\rm F}(W_{\rm F})}{P_{\rm R}(-W_{\rm F})} = e^{\beta(W_{\rm F} - \Delta F)}. \tag{4}$$

Note that the two distributions intersect at $W_{\rm F} = \Delta F$. Multiplying both sides of the above equation by $\exp(-\beta W_{\rm F})$, and noting that $P_{\rm R}(-W_{\rm F})$ is normalized to unity, one recovers the Jarzynski equality.

Our model. – Our model comprises N interacting particles, labelled $i = 1, 2, \ldots, N$, moving on a unit circle. Let the angle $\theta_i \in [0, 2\pi)$ denote the location of the i-th particle on the circle. A microscopic configuration of the system is $\mathcal{C} \equiv \{\theta_i; i = 1, 2, \ldots, N\}$. The particles interact through a long-range potential $\mathcal{V}(\mathcal{C}) \equiv K/(2N) \sum_{i,j=1}^{N} [1 - \cos(\theta_i - \theta_j)]$, with K being the coupling constant that we take to be unity in the following

to consider an attractive interaction[1]. An external field of strength h produces a potential $\mathcal{V}_{\rm ext}(\mathcal{C}) \equiv -h\sum_{i=1}^{N}\cos\theta_i$; thus, the total potential energy is $V(\mathcal{C}) \equiv \mathcal{V}(\mathcal{C}) + \mathcal{V}_{\rm ext}(\mathcal{C})$. The external field breaks the rotational invariance of $\mathcal{V}(\mathcal{C})$ under equal rotation applied to all the particles.

The dynamics of the system involves configurations evolving according to a stochastic Monte Carlo (MC) dynamics. Every particle in a small time $\mathrm{d}t \to 0$ attempts to hop to a new position on the circle. The i-th particle attempts with probability p to move forward (in the anti-clockwise sense) by an amount ϕ; $0 < \phi < 2\pi$, so that $\theta_i \to \theta_i' = \theta_i + \phi$, while with probability $q = 1-p$, it attempts to move backward by the amount ϕ, so that $\theta_i \to \theta_i' = \theta_i - \phi$. In either case, the particle takes up the attempted position with probability $g(\Delta V(\mathcal{C}))\mathrm{d}t$. Here, $\Delta V(\mathcal{C})$ is the change in the potential energy due to the attempted hop from θ_i to θ_i': $\Delta V(\mathcal{C}) = (1/N)\sum_{j=1}^{N}[-\cos(\theta_i' - \theta_j) + \cos(\theta_i - \theta_j)] - h[\cos\theta_i' - \cos\theta_i]$. The dynamics does not preserve the ordering of particles on the circle. The function g has the form $g(z) = (1/2)[1 - \tanh(\beta z/2)]$, where β is the inverse temperature. Such a form of $g(z)$ ensures that for $p = 1/2$, when the particles jump symmetrically forward and backward, the stationary state of the system is the canonical equilibrium state at inverse temperature β (see footnote [2]). The case $p \neq q$ mimics the effect of an external drive on the particles to move in one preferential direction along the circle. The field strength h has the role of the externally controlled parameter λ discussed in the preceding section.

The model was introduced in ref. [12] as an LRI system evolving under MC dynamics. Depending on the parameters in the dynamics, the system relaxes to either a canonical equilibrium state or a NESS. In either case, the single-particle phase space distribution can be solved *exactly* in the thermodynamic limit.

A model that has been much explored in the recent past to study static and dynamic properties of LRI systems is the so-called Hamiltonian mean-field (HMF) model [9]. This model involves N particles moving on a circle, interacting via a long-range potential with the same form as $\mathcal{V}(\mathcal{C})$, and evolving under deterministic Hamilton dynamics. The dynamics leads at long times to an equilibrium stationary state. Our model may be looked upon as a generalization of the microcanonical dynamics of the HMF model to a stochastic dissipative dynamics in the overdamped regime, with an additional external drive causing a biased motion of the particles on the circle. The dissipation mimics the interaction of the system with an external heat bath.

In the Fokker-Planck limit $\phi \ll 1$, we may in the thermodynamic limit $N \to \infty$ consider, in place of the N-particle dynamics described above, the motion of a single particle in a self-consistent mean field generated by its interaction with all the other particles. The dynamics of the particle is described by the Langevin equation [12]

$$\dot{\theta} = (2p-1)\phi - \frac{\phi^2\beta}{2}\frac{\mathrm{d}\langle v\rangle}{\mathrm{d}\theta} + \phi\eta(t), \tag{5}$$

where the dot denotes differentiation with respect to time, and $\eta(t)$ is a Gaussian, white noise with $\overline{\eta(t)} = 0$, $\overline{\eta(t)\eta(t')} = \delta(t-t')$. Here, overbars denote averaging over noise realizations. In eq. (5), $\langle v\rangle \equiv \langle v\rangle[\rho](\theta,t) \equiv -m_x[\rho]\cos\theta - m_y[\rho]\sin\theta - h\cos\theta$ is the mean-field potential, with $(m_x[\rho], m_y[\rho]) \equiv \int \mathrm{d}\theta\ (\cos\theta, \sin\theta)\rho(\theta,t)$, where $\rho(\theta,t)$ is the probability density of the particle to be at location θ on the circle at time t. Together with $\rho(\theta,t) = \rho(\theta+2\pi,t)$, and the normalization $\int_0^{2\pi}\mathrm{d}\theta\ \rho(\theta,t) = 1\ \forall\ t$, $\rho(\theta,t)$ is a solution of the Fokker-Planck equation [12]

$$\frac{\partial\rho}{\partial t} = -\frac{\partial}{\partial\theta}\left[\left((2p-1)\phi - \frac{\phi^2\beta}{2}\frac{\mathrm{d}\langle v\rangle}{\mathrm{d}\theta}\right)\rho\right] + \frac{\phi^2}{2}\frac{\partial^2\rho}{\partial\theta^2}. \tag{6}$$

Steady state. – Let $P(\mathcal{C},t)$ be the probability to observe configuration $\mathcal{C}$ at time t. At long times, the system relaxes to a stationary state corresponding to time-independent probabilities $P_{\rm st}(\mathcal{C})$. For $p = 1/2$, the system has an equilibrium stationary state in which the condition of detailed balance is satisfied, and $P_{\rm st}(\mathcal{C})$ is given by the canonical equilibrium measure $P_{\rm eq}(\mathcal{C}) \propto e^{-\beta V(\mathcal{C})}$. On the other hand, for $p \neq 1/2$, the system at long times reaches a NESS, which is characterized by a violation of detailed balance that leads to closed loops of net non-zero probability current in the phase space.

For the single-particle dynamics (5), the stationary solution $\rho_{\rm ss}$ of eq. (6) is given by [12]

$$\rho_{\rm ss}(\theta;h) = \frac{\rho_{\rm ss}(0;h)}{e^{g(\theta)}}\left[1 + (e^{-\frac{4\pi(2p-1)}{\phi}} - 1)\frac{A(\theta)}{A(2\pi)}\right]; \tag{7}$$

$g(\theta) \equiv -2(2p-1)\theta/\phi + \beta\langle v\rangle[\rho_{\rm ss}](\theta)$, $A(\theta) \equiv \int_0^{\theta}\mathrm{d}\theta' e^{g(\theta')}$, while the constant $\rho_{\rm ss}(0;h)$ is fixed by the normalization $\int_0^{2\pi}\mathrm{d}\theta\ \rho_{\rm ss}(\theta;h) = 1\ \forall\ h$. To show the effectiveness of the single-particle dynamics in describing the stationary state of the N-particle dynamics for large N and for $\phi \ll 1$, fig. 1 shows a comparison between the result (7) and MC simulation results for the N-particle dynamics with $N = 500, \phi = 0.1$, demonstrating an excellent agreement.

For $p = 1/2$, eq. (7) gives the equilibrium single-particle distribution $\rho_{\rm eq}(\theta;h) = e^{-\beta\langle v\rangle[\rho_{\rm eq}](\theta)}/Z(h)$, with $Z(h) \equiv \int_0^{2\pi}\mathrm{d}\theta\ \rho_{\rm eq}(\theta;h) = 2\pi I_0(\beta m_{\rm eq})$, and $I_n(x)$ the modified Bessel function of order n. Here, $m_{\rm eq} \equiv \sqrt{(m_x^{\rm eq}+h)^2 + (m_y^{\rm eq})^2}$ is obtained by solving the transcendental equation $m_{\rm eq} + h = I_1(\beta m_{\rm eq})/I_0(\beta m_{\rm eq})$, see [9].

[1]The exponent α characterizing the decay of the inter-particle potential with separation is zero here, thus corresponding to the extreme case of long-range interactions, when the potential does not decay at all with distance.

[2]Non-additivity of LRI systems brings in complications in deriving the canonical equilibrium while starting from a microcanonical one, whereby the former describes fluctuations in a subsystem that is a part of and is in interaction with the rest of the system. We however invoke canonical equilibrium in the sense that although non-additive, an LRI system in contact with an external short-ranged heat bath via a small coupling will be in canonical equilibrium at a temperature given by that of the bath [11].

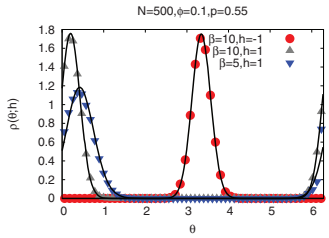

Fig. 1: (Colour online) Stationary distribution $\rho_{\rm ss}(\theta;h)$ for $p \neq 1/2$: a comparison between MC simulation results (points) for $\phi = 0.1, N = 500$ and three values of field h, and the theoretical result (continuous lines) in the Fokker-Planck approximation in the limit $N \to \infty$ given by eq. (7) illustrates an excellent agreement.

For $h = 0$, $m_{\rm eq}$ as a function of β decreases continuously from unity at $\beta = \infty$ to zero at the critical value $\beta_c = 2$, and remains zero at smaller β, thus showing a second-order phase transition at β_c [9]. For $h \neq 0$, the magnetization is non-zero at all β, hence, there is no phase transition.

Equilibrium initial condition. – Let us consider $p = 1/2$ in our model, when the system at a fixed value of h has an equilibrium stationary state. In the following, we measure time in units of MC steps, where one MC step corresponds to N attempted hops of randomly chosen particles. Starting with the system in equilibrium at $h = h_0$, we perform MC simulations of the dynamics while changing the field strength linearly over a total time $\tau \in \mathbb{I}$, with $\tau \ll \tau_{\rm eq}$, such that at the α-th time step, the field value is $h_\alpha = h_0 + \Delta h\ \alpha/\tau;\ \alpha \in [0,\tau]$. Here, Δh is the total change in the value of the field over time τ. Note that the FRs are expected to hold for arbitrary protocols $\{\lambda(t)\}$; the linear variation we consider is just a simple choice. Here, $\tau_{\rm eq}$ is the typical equilibration time at a fixed value of h, and the condition $\tau \ll \tau_{\rm eq}$ ensures that the system during the thermodynamic transformation is driven arbitrarily far from equilibrium. The initial equilibrium configuration is prepared by sampling independently each θ_i from the single-particle distribution $\rho_{\rm eq}(\theta;h)$, with $m_{\rm eq}$ determined by solving $m_{\rm eq} + h_0 = I_1(\beta m_{\rm eq})/I_0(\beta m_{\rm eq})$. The work done on the system during the evolution is [3]

$$W_{\rm F} \equiv \int_0^\tau \frac{\partial V}{\partial h}\dot{h}\,{\rm d}t = -\frac{1}{\tau}\sum_{\alpha=1}^{\tau}\sum_{i=1}^{N}\cos\theta_i^{(\alpha)}, \qquad (8)$$

where $\theta_i^{(\alpha)}$ is the angle of the i-th particle at the α-th time step of evolution. In another set of experiments, we prepare the system to be initially in equilibrium at $h = h_\tau$, and then evolve the system while decreasing the field strength linearly in time as $h_\alpha = h_\tau - \Delta h\ \alpha/\tau$. During these forward and reversed protocols of changing the field, we compute the respective work distributions $P_{\rm F}(W_{\rm F})$ and $P_{\rm R}(W_{\rm R})$, for $\phi \ll 1$ and a number of system sizes $N \gg 1$. We take $\tau_{\rm eq} = N^2$, confirming that the distributions $P_{\rm F}(W_{\rm F})$ and $P_{\rm R}(W_{\rm R})$ do not change appreciably by considering $\tau_{\rm eq}$ larger than N^2.

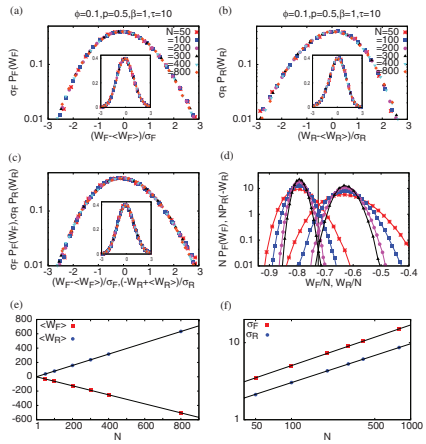

Fig. 2: (Colour online) Starting with an initial equilibrium state at inverse temperature $\beta = 1$ and field $h = h_0 = 1.0$, and then increasing the field linearly in time to $h = 2.0$ over a time $\tau = 10$ Monte Carlo steps (thus, $\Delta h = 1.0$), panel (a) shows the scaled work distribution for this forward (F) protocol, while (b) shows the same for the corresponding reverse (R) protocol, both for a range of system sizes N. Scaling collapse in (c) suggests for the scaling functions in (a) and (b) the symmetry $g_{\rm F}(x) = g_{\rm R}(-x)$. Panel (d) shows $NP_{\rm F}(W_{\rm F})$ (right set of curves) and $NP_{\rm R}(W_{\rm R})$ (left set) as a function of $W_{\rm F}/N$ and $W_{\rm R}/N$, respectively, for different N, with the curves intersecting at a value given by the free-energy difference per particle Δf estimated using eq. (11) for single-particle equilibrium. Panels (e) and (f) show, respectively, the dependence of the average and the standard deviation of the forward and the reverse work on N, suggesting that while the average grows linearly with N, one has $\sigma_{\rm F} \sim N^a;\ a \approx 0.528$, and $\sigma_{\rm R} \sim N^b;\ b \approx 0.504$. Here, $\phi = 0.1, p = 0.5$.

Figures 2(a), (b) show the forward and the reverse work distribution for a range of system sizes N. Here, we have taken $\phi = 0.1, h_0 = 1.0, \tau = 10, \beta = 1, \Delta h = 1.0$. The data collapse evident from the plots suggests the scaling

$$P_{\rm B}(W_{\rm B}) \sim \frac{1}{\sigma_{\rm B}} g_{\rm B}\left(\frac{W_{\rm B} - \langle W_{\rm B}\rangle}{\sigma_{\rm B}}\right); \quad {\rm B} \equiv {\rm F,R}, \qquad (9)$$

where $g_{\rm B}$ is the scaling function, while $\langle W_{\rm B}\rangle$ and $\sigma_{\rm B}$ are, respectively, the average and the standard deviation of the work. A similar scaling, termed the Bramwell-Holdsworth-Pinton (BHP) scaling, was first observed in the context of fluctuations of injected power in confined turbulence and magnetization fluctuations at the critical point of a ferromagnet [13]. Over the years, a similar scaling has been reported in a wide variety of different contexts, from models of statistical physics, such as Ising and percolation models, sandpiles, granular media in a self-organized critical state [14], to fluctuations in river level [15], and even in fluctuations in short electrocardiogram episodes in humans [16]. Here, the BHP scaling is shown for the first time to also hold for work distributions out of equilibrium. The dependence of the average and the standard deviation on the system size N is shown in panels (e) and (f), respectively, with the numerically data suggesting that

$\langle W_{\rm B}\rangle \propto N$, $\sigma_{\rm F} \sim N^a$; $a \approx 0.528$, and $\sigma_{\rm R} \sim N^b$; $b \approx 0.504$. The data collapse in (c) suggests the remarkable symmetry

$$g_{\rm F}(x) = g_{\rm R}(-x). \tag{10}$$

An understanding of the origin of this symmetry, and particularly, whether it is specific to our model or holds in general, is left for future work. Figure 2(d) shows the distribution of the work per particle. Two essential features of the plots are evident, namely, i) significant fluctuations of the work values even for large system size, and ii) the forward and the reverse distribution intersecting at a common value regardless of the system size. By virtue of the Crooks theorem (4), this common value should be given by the free-energy difference per particle Δf between the canonical equilibrium states of the system at field values h_τ and h_0. This latter quantity may be computed theoretically by knowing the free energy per particle in the limit $N \to \infty$ and at a fixed value of h [9]:

$$f(h) = \frac{1}{2}m_{\rm eq}^2 - \frac{1}{\beta}\ln\left(\int {\rm d}\theta\, e^{\beta[(m_x^{\rm eq}+h)\cos\theta + m_y^{\rm eq}\sin\theta]}\right). \tag{11}$$

Using the above gives $\Delta f \approx 0.725$, which is seen in fig. 2(d) to match very well with the intersection point of the forward and the reverse distribution of the work.

While fig. 2 was for inhomogeneous initial equilibrium, in order to validate our results also for homogeneous initial conditions, fig. 3 repeats the plots at $h_0 = 0.0$ and at a temperature larger than $1/\beta_c$. In this case, the scaled work distributions fit quite well to a Gaussian distribution with zero average and unit standard deviation, see figs. 3(a), (b), so that $g(x) = \exp(-x^2/2)/\sqrt{2\pi}$, and, therefore, the symmetry (10) is obviously satisfied. The free-energy difference Δf can be estimated by using eq. (11), but can also be obtained by using eq. (4) and the fact that in the present situation, the scaled work distributions are Gaussian. Using the latter procedure, one gets the expression $\Delta f = (\langle W_{\rm F}\rangle - \langle W_{\rm R}\rangle)/(2N)$ [17]; then, on substituting our numerical values for $\langle W_{\rm F}\rangle$ and $\langle W_{\rm R}\rangle$, we get $\Delta f \approx 0.161$. In fig. 3(c), we show that this value of Δf coincides with the point of intersection of the forward and the reverse work distribution.

In figs. 2 and 3, it may be seen that $\sigma_{\rm F} > \sigma_{\rm R}$, and also $\langle W_{\rm R}\rangle > |\langle W_{\rm F}\rangle|$. In computing $\sigma_{\rm F}$, we start with a smaller magnetized state (thus, with the particles more spread out on the circle) than the state we start with in computing $\sigma_{\rm R}$. As a result, the work done in the former case during the thermodynamic transformation in which the increasing field tries to bring the particles closer together will show more variation from one particle to another, resulting in $\sigma_{\rm F} > \sigma_{\rm R}$. Now, $\langle W\rangle$, either F or R, is basically the time-integrated magnetization, see eq. (8). During the forward process, we start with a less-magnetized equilibrium state with magnetization $m_0^{\rm eq}$, and then increase the field for a finite time. The final magnetization value $m_{\rm fin,F}$ reached thereby will be smaller than the actual equilibrium value $m_1^{\rm eq}$ for the corresponding value of the field, since we did not allow the system to equilibrate during the transformation. For the reverse process, we started with this equilibrium value $m_1^{\rm eq}$, and during the transformation when the field is decreased, the magnetization decreases but not substantially to the value $m_0^{\rm eq}$, since the system remains out of equilibrium during the transformation. As a result, the time-integrated forward magnetization, whose mean value is $\langle W_{\rm F}\rangle$, is smaller in magnitude than the time-integrated reverse magnetization, whose mean value is $\langle W_{\rm R}\rangle$. In fig. 3, $\langle W_{\rm F}\rangle$ is very close to zero. This is because here, we start with a homogeneous equilibrium for which the magnetization value is $m_0^{\rm eq} = 0$, and then increase the field for a finite time to a not-so-high value $h = 1$, so the magnetization does not increase much from the initial value. Hence, $\langle W_{\rm F}\rangle$, which is the time-integrated magnetization during this forward transformation, is close to zero.

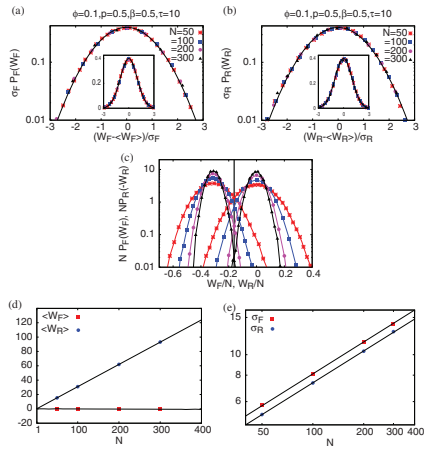

Fig. 3: (Colour online) Plots similar to those in fig. 2, but with $\beta = 0.5, h_0 = 0.0, \tau = 10, \Delta h = 1.0$. The black lines in panels (a) and (b) denote a Gaussian distribution with zero average and unit standard deviation. While the averages in (d) grow linearly with N, the standard deviations in (e) satisfy $\sigma_{\rm F} \sim N^a$; $a \approx 0.501$, and $\sigma_{\rm R} \sim N^b$; $b \approx 0.5$.

Figures 2 and 3, while illustrating the validity of the Crooks theorem (and hence, of the Jarzynski equality) for many-body stochastic LRI systems, underline the effective single-particle nature of the actual N-particle dynamics for large N in the Fokker-Planck limit $\phi \ll 1$. This feature is further illustrated by our analysis of fluctuations while starting from NESSs, as we now proceed to discuss.

Non-equilibrium initial condition. – We now consider $p \neq 1/2$ in our model. In this case, the system at a fixed value of h relaxes to a NESS. We wish to compute the distribution of the quantity Y appearing in the Hatano-Sasa equality (2). To proceed, we consider a large value of N and $\phi \ll 1$ and use a combination of N-particle dynamics, and the knowledge of the single-particle stationary-state distribution (7). Starting with the initial value $h = h_0$, the field is varied linearly in time, as in the equilibrium case; specifically, at the α-th time

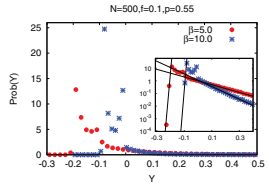

Fig. 4: (Colour online) Starting with initial conditions in a NESS at $h = h_0 = 1.0$, and then increasing the field linearly in time to $h = 1.15$ over $\tau = 15$ Monte Carlo steps (thus, $\Delta h = 0.15$), the figure shows for two values of initial inverse temperature β the distribution of the quantity Y appearing in the Hatano-Sasa equality (2). The black lines in the inset stand for the exponential fit $\sim \exp(aY)$ to the left tail, with $a \approx 280$ for $\beta = 5$ and $a \approx 300$ for $\beta = 10$, and the exponential fit $\sim \exp(-bY)$ to the right tail, with $b \approx 7$ for $\beta = 5$ and $b \approx 11.5$ for $\beta = 10$. Here, $N = 500, \phi = 0.1, p = 0.55$.

step, the field is $h_\alpha = h_0 + \Delta h\ \alpha/\tau;\ \alpha \in [0, \tau]$. Again, the choice of the protocol is immaterial in as far as validity of the Hatano-Sasa equality is concerned. The steps in computing the Y-distribution for fixed values of $\beta, h_0, \Delta h, \tau$ are as follows. A state prepared by sampling independently each θ_i uniformly in $[0, 2\pi)$ is allowed to evolve under the N-particle MC dynamics with $h = h_0$ to eventually relax to the stationary state, which is confirmed by checking that the resulting single-particle distribution is given by eq. (7). Subsequently, the particles are allowed to evolve under the time-dependent field h_α for a total time τ, and the quantity Y is computed along the trajectory of each particle according to eq. (1), which is given in the present case for the i-th particle by the following expression, as an approximation to the integral and the derivative appearing in eq. (1):

$$Y_i = \sum_{\alpha=1}^{\tau} \ln\left(\frac{\rho_{\rm ss}(\theta_i^{(\alpha)}; h_{\alpha-1})}{\rho_{\rm ss}(\theta_i^{(\alpha)}; h_\alpha)}\right), \qquad (12)$$

where $\{\theta_i^{(\alpha)}\}_{0\le\alpha\le\tau}$ gives the trajectory of the i-th particle, and $\rho_{\rm ss}(\theta_i^{(\alpha)}; h_\alpha)$ is computed by using eq. (7). Repeating these steps yields the distribution of Y for each particle, which is finally averaged over all the particles to obtain the distribution $P(Y)$ depicted in fig. 4. Here, we use two values of β, while the other parameters are $p = 0.55, N = 500, \phi = 0.1, h_0 = 1.0, \Delta h = 0.15, \tau = 15$. As is evident from the figure, the distribution is highly asymmetric, and in particular, has exponential tails (see the inset). From the data for $P(Y)$, we find for $\langle \exp(-Y)\rangle$ the value 1.04 for $\beta = 10$, and the value 1.11 for $\beta = 5$, which within numerical accuracy are consistent with the expected value of unity. Let us reiterate the combined use of the N-particle dynamics and the exact single-particle stationary state distribution in obtaining the Y-distribution, and remark that the consistency of the final results with the Hatano-Sasa equality further highlights the effective mean-field nature of the N-particle dynamics for large N.

To conclude, in this work, we studied the out-of-equilibrium fluctuations of the work done by a time-dependent external force on a many-particle system with long-range interactions and evolving under stochastic dynamics. For both equilibrium and non-equilibrium initial conditions, we characterized the fluctuations, and revealed how a simpler single-particle Langevin dynamics in a mean field gives accurate quantitative predictions for the N-particle dynamics for large N. This, in turn, highlights the effective mean-field nature of the original many-particle dynamics for large N. It is interesting to generalize recent studies of work statistics in quantum many-body short-range systems, *e.g.*, [18,19], to those with long-range interactions, and unveil any effective mean-field description.

* * *

SG and SR thank the ENS de Lyon for hospitality. We acknowledge fruitful discussions with A. C. Barato, M. Baiesi, S. Ciliberto, G. Jona-Lasinio, and A. Naert.

REFERENCES

[1] Kubo R., *Rep. Prog. Phys.*, **29** (1966) 255.
[2] Seifert U., *Rep. Prog. Phys.*, **75** (2012) 126001.
[3] Jarzynski C., *Phys. Rev. Lett.*, **78** (1997) 2690.
[4] Crooks G., *Phys. Rev. E*, **60** (1999) 2721.
[5] Hatano T. and Sasa S., *Phys. Rev. Lett.*, **86** (2001) 3463.
[6] Bustamante C. *et al.*, *Phys. Today*, **58**, issue No. 7 (2005) 43.
[7] Collin D. *et al.*, *Nature*, **437** (2005) 231.
[8] Trepagnier E. H. *et al.*, *Proc. Natl. Acad. Sci. U.S.A.*, **101** (2004) 15038.
[9] Campa A. *et al.*, *Physics of Long-range Interacting Systems* (Oxford University Press, UK) 2014.
[10] Bertini L. *et al.*, *J. Stat. Mech.* (2015) P10018.
[11] Baldovin F. and Orlandini E., *Phys. Rev. Lett.*, **96** (2006) 240602.
[12] Gupta S. *et al.*, *J. Stat. Mech.* (2013) P11003.
[13] Bramwell S. T. *et al.*, *Nature*, **396** (1998) 552.
[14] Bramwell S. T. *et al.*, *Phys. Rev. Lett.*, **84** (2000) 3744.
[15] Bramwell S. T. *et al.*, *Europhys. Lett.*, **57** (2002) 310.
[16] Bakucz P. *et al.*, *Acta Polytech. Hung.*, **11** (2014) 73.
[17] Douarche F. *et al.*, *J. Stat. Mech.* (2005) P09011.
[18] Russomanno A. *et al.*, *J. Stat. Mech.* (2015) P08030.
[19] Dutta A. *et al.*, *Phys. Rev. E*, **92** (2015) 012104.